Screening in compensated semiconductors

R Grill

Institute of Physics, Charles University, Ke Karlovu 5, CZ-121 16 Prague 2, Czech Republic

Abstract. Mutual screening of charged impurities in bulk compensated semiconductors is described. Several models for analytical treatment are discussed. Monte Carlo simulations of impurity relaxation in disordered systems at non-zero temperatures are performed. Pair distribution functions are obtained. A structure of the screened acceptor–donor-electron complex is studied. Friedel-like oscillations in a screening charge distribution are observed. The matrix element for electron scattering and electron mobility is calculated. Remarkable behaviour at small wavevectors is observed. Essential corrections against standard models at the limit of zero temperature are found.

1. Introduction

Screening of the electron–charged-impurity interaction is often discussed in the literature. Mostly it is based on a theory of screening of the interaction by free carriers surrounding random distributed positive and negative charged impurities. However, in compensated semiconductors, especially at low temperatures when the free carriers freeze out, the screening is given predominantly by a rearrangement and mutual screening of positive (n-type) or negative (p-type) charges. This effect has not been so widely investigated and the theoretical description is not satisfactory.

Reviewing longstanding contributions to the problem there have been two attempts to solve that—Conwell and Weisskopf [1] and Brooks and Herring [2]. A main qualitative drawback of these models is caused by too large screening of the Coulomb interaction at low temperature which results in an infinite limit of electron mobility at $T \to 0$. A more recent paper of Falicov and Cuevas [3] removes this fault introducing pair impurity correlation functions. However, the given analysis contains several simplifications to make the analytical treatment possible. Thus the relevance of the submitted theory is decreased and additional improvement should be performed. Another procedure based on Fujita formalism [4, 5] of a collisional broadening of the spectral function has been used in [6]. Both the latter papers yield a zero limit of electron mobility at $T \to 0$. The mentioned literature is limited to the few ancient entries above as I have not found any substantial paper on the problem in the recent literature.

The aim of this paper is to extend and precise the theory from [3]. Computer simulations offer a numerical form of pair correlation functions which allow us to calculate the electron mobility in a limit of relaxation time approximation without additional simplifications.

2. Theory

Throughout the paper we shall assume an n-type non-degenerate semiconductor with N_d donors and N_a acceptors per unit volume ($N_d > N_a$). The following notation is used

throughout this paper: N_d^+ (N_a^-) means the average density of ionized donors (acceptors), $\mathcal{N}_d^+(r)$ ($\mathcal{N}_a^-(r)$) designates the local density of ionized donors (acceptors), n_e ($\mathcal{N}_e(r)$) is the average (local) density of free electrons. e, $\varphi(r)$, ε_s, ε_0 and Ω are respectively the charge of the electron, electric potential, static and vacuum dielectric constant and volume of the sample. We set $\varepsilon_s = 15$ in calculations. All acceptors are ionized and free holes are neglected here. As it is usual in screening calculations we start with the Poisson equation

$$\nabla^2 \varphi = -\frac{e}{\varepsilon_0 \varepsilon_s} \left[\mathcal{N}_e(r) + \mathcal{N}_a^-(r) - \mathcal{N}_d^+(r) \right]. \tag{1}$$

Positively charged donors are neglected. We assume that free carriers play a small role at the screening of compensated non-degenerate material. Thus, we describe them only by a simple linear expansion in $\varphi(r)$ which is valid at high enough temperature T or non-degenerate independent carriers, smooth potential and low particle concentration.

$$\mathcal{N}_e(r) = n_e \exp\left[-\frac{e\varphi(r)}{k_B T}\right] \approx n_e \left[1 - \frac{e\varphi(r)}{k_B T}\right]. \tag{2}$$

In case of screening at low temperature when free carriers freeze out n_e can be set to zero. Following [3] we mark y_l; $l = 1, 2, 3, \ldots, \mathcal{N}_a \Omega$ coordinates of acceptors and z_s; $s = 1, 2, 3, \ldots, \mathcal{N}_d^+ \Omega$ coordinates of ionized donors. Crossing to the Fourier transform we write

$$\mathcal{N}_a^-(r) = \sum_l \delta(r - y_l) = \sum_{k,l} \exp\left[ik \cdot (r - y_l)\right] \tag{3}$$

and similarly for the donors. Equation (1) is then in the form

$$\left(k^2 + \frac{1}{d_d^2}\right) \Phi(k) = \frac{e}{\varepsilon_0 \varepsilon_s} \left[\sum_l \exp\left(-ik \cdot y_l\right) - \sum_s \exp\left(-ik \cdot z_s\right) + n_e \delta_{k,0} \right] \tag{4}$$

where

$$d_d^2 = \frac{\varepsilon_0 \varepsilon_s k_B T}{e^2 n_e} \tag{5}$$

is the free-electron screening length. The square of the matrix element for the electron scattering for $k \neq 0$ is given by

$$|M(k)|^2 = \left|\frac{e}{\Omega} \Phi(k)\right|^2 = \left[\frac{e^2}{\varepsilon_0 \varepsilon_s \Omega \left(k^2 + d_d^{-2}\right)}\right]^2 \left\{\left\langle\!\left\langle \sum_{ll'} \exp\left[ik \cdot (y_l - y_{l'})\right] \right\rangle\!\right\rangle \right.$$

$$\left. + \left\langle\!\left\langle \sum_{ss'} \exp\left[ik \cdot (z_s - z_{s'})\right] \right\rangle\!\right\rangle - 2\left\langle\!\left\langle \sum_{ls} \cos\left[k \cdot (y_l - z_s)\right] \right\rangle\!\right\rangle \right\}. \tag{6}$$

$\langle\!\langle \cdots \rangle\!\rangle$ means an ensemble averaging. Treating the macroscopically uniform and isotropic system we can average over a sphere obtaining direction-independent quantities

$$|M(k)|^2 = \left[\frac{e^2}{\varepsilon_0 \varepsilon_s \left(k^2 + d_d^{-2}\right)}\right]^2 \frac{1}{\Omega} F(k) \tag{7}$$

where

$$F(k) = N_a + N_d^+ + \frac{4\pi}{\Omega k} \int_0^\infty r \sin kr \left[C_{aa}(r) + C_{dd}(r) - 2C_{ad}(r)\right] dr. \tag{8}$$

C_{aa}, C_{dd}, C_{ad} are respectively acceptor–acceptor, donor–donor and acceptor–donor pair distribution functions given by

$$C_{aa}(r) = \left\langle\!\left\langle \sum_{\substack{ll'\\l\neq l'}} \delta(r - y_l + y_{l'}) \right\rangle\!\right\rangle$$

$$C_{dd}(r) = \left\langle\!\left\langle \sum_{\substack{ss'\\s\neq s'}} \delta(r - z_s + z_{s'}) \right\rangle\!\right\rangle \tag{9}$$

$$C_{ad}(r) = \left\langle\!\left\langle \sum_{ls} \delta(r - y_l + z_s) \right\rangle\!\right\rangle.$$

If we assume that there is no correlation in the distribution of the impurity atoms, the C_{aa} can be neglected. Thus it has only formal meaning in this paper. The integral in (8) expresses the screening caused by a rearrangement of the charge on the donor sites. In the case of no correlations it is equal to zero. The widely used model of Brooks and Herring [2] sets $F(k) = N_a + N_d^+$ and grasps the total screening by a change of the electron concentration n_e at (5) by an effective concentration

$$n_e^* = n_e + (n_e + N_a)\left[1 - (n_e + N_a)/N_d\right]. \tag{10}$$

A form similar to (7) was also obtained in [3]. Free-particle and donor–donor screenings were excluded there. We shall try to avoid this simplification in this paper.

The acceptors are fully screened by the charged donors and free electrons. The screening charge must be collected at the distant part of the volume. The mobile charges screen the acceptors and interact mutually. Simultaneously the system must be neutral. If T or n_e are low, the acceptors are screened mainly by the donors. Each acceptor serves as a centre to give rise to a complex structure containing on average N_d^+/N_a donors and n_e/N_a electrons. If T and n_e increase, some donors and the same number of electrons escape from the complex. Then the free electrons (or a lack of them on the acceptors) start to prevail in the screening of the interaction. These conditions provide rules to establish some properties of the correlation functions. The requirement of neutrality gives for the long-range branch of the functions

$$-C_{aa}(\infty) + C_{ad}(\infty) - C_{ae}(\infty) = 0$$
$$-C_{ad}(\infty) + C_{dd}(\infty) - C_{de}(\infty) = 0 \tag{11}$$
$$-C_{ae}(\infty) + C_{de}(\infty) - C_{ee}(\infty) = 0.$$

The index e means the electrons. The correlation functions are then found in the form

$$C_{aa}(\infty) = N_a\left(N_a\Omega - 1\right)$$
$$C_{ad}(\infty) = N_d^+\left(N_a\Omega - X\right)$$
$$C_{ae}(\infty) = N_a\left(n_e\Omega + 1\right) - N_d^+ X$$
$$C_{dd}(\infty) = N_d^+\left(-\frac{N_d^+}{N_a}X^2 + X + N_d^+\Omega - 1\right) \tag{12}$$
$$C_{de}(\infty) = N_d^+\left(-\frac{N_d^+}{N_a}X^2 + 2X + n_e\Omega - 1\right)$$
$$C_{ee}(\infty) = N_d^+\left(-\frac{N_d^+}{N_a}X^2 + 3X - 1\right) - N_a + n_e^2\Omega$$

where $X \in (0, 1)$ is a fraction of donors bound in the complexes. The function $F(k \to 0)$ (8) gives

$$F(k \to 0) = N_a + N_d^+ \left(1 - 3X + \frac{N_d^+}{N_a} X^2\right). \tag{13}$$

X cannot be established from the above conditions and must be deduced from a detailed calculation.

Due to the fact that any constant function gives no increment to the integral in (8), it is useful to substitute C_{aa}, C_{dd} and C_{ad} by the difference functions

$$\delta C_{aa}(r) = C_{aa}(r) - C_{aa}(\infty) = 0$$
$$\delta C_{dd}(r) = C_{dd}(r) - C_{dd}(\infty) \tag{14}$$
$$\delta C_{ad}(r) = C_{ad}(r) - C_{ad}(\infty).$$

which describe short-range correlations. For the sake of abbreviation we introduce the total screening function

$$\delta C_{tot} = 2\delta C_{ad} - \delta C_{aa} - \delta C_{dd}. \tag{15}$$

The introduction of the difference function allows us to limit the radial integration to a range where the screening effects are really observed.

Since all acceptors are assumed ionized, and only a fraction N_d^+/N_d of the total number of donors is ionized, we would expect the donors to be preferentially ionized in those locations which are close to acceptor sites. This means that in the neighbourhood of an acceptor the density of ionized donors should reach the value N_d [3]. Similarly there are no pairs of ionized donors in a close proximity. Thus

$$C_{dd}(r \to 0) = 0 \qquad C_{ad}(r \to 0) = N_a N_d \Omega. \tag{16}$$

Finding the correlation functions is a crucial point of the reported investigation. Here we outline two possibilities for how to solve the problem analytically.

2.1. Exponential correlation

Seeking the correlation function in an exponential form is useful for a simple analytical treatment which allows us to obtain analytical forms as both for relaxation time and for electron mobility. The model was introduced first in [3] where the donor–donor correlations were omitted. We generalize the approach including these correlations. Here as well as in the next model we neglect n_e and set $d_d^{-2} = 0$. Further we assume large volume $\Omega N_d \gg 1$. The correlation function is looked for in the form

$$\delta C_{tot}(r) = \alpha \Omega \exp(-ar) \tag{17}$$

where

$$\alpha = \left[2N_a \left(N_d - N_d^+\right) + \left(N_d^+\right)^2\right]. \tag{18}$$

The pre-exponential term is obtained from the condition (16). Due to the fact that the interaction must be fully screened at large distances we have an additional condition $F(k \to 0) = 0$ to find the parameter a

$$a^3 = \frac{8\pi\alpha}{N_a + N_d^+}. \tag{19}$$

However, there is no serious reason to take the function δC_{tot} as in (17). As seen later especially at low temperature the exponential form differs from the correct functions.

2.2. Dipole model

If the compensation is low ($N_a \ll N_d$) then at low temperature, charged donors are localized at the minimal distance from the acceptors. Their positions are given just by a possibility of reaching the close proximity of the acceptors and there is thus no donor–donor correlation ($\delta C_{dd} = 0$). The scattering potential can be described by a set of randomly distributed dipoles. The distribution function of the dipoles is given by

$$\delta C_{ad}(r) = N_d \left[1 - 4\pi \int_0^r x^2 \, \delta C_{ad}(x) \, dx \right]. \tag{20}$$

At small distances the dipole distribution is given by the total donor concentration. Increasing the distance the dipole is created only in the case where there is no closer configuration. The second term in the angular brackets expresses a probability that up to the distance r the dipole has already been created. The solution of (20) reads

$$\delta C_{ad}(r) = N_d \exp\left(-\frac{4}{3}\pi N_d r^3 \right). \tag{21}$$

Similarly as in the case of the exponential correlation we could try to generalize (21) to a higher compensation degree writing

$$\delta C_{tot}(r) = \alpha\Omega \exp(-b r^3) \tag{22}$$

$$b = \frac{4\pi\alpha}{3\left(N_a + N_d^+\right)}. \tag{23}$$

The ensuing numerical treatment will be fruitful to check correctness of the performed generalization at higher compensations.

3. Monte Carlo simulations

Numerical simulations of the impurity band and the charge relaxation are currently discussed in the literature [7, 8]. They are directed mostly at studying a single-particle density of states in the impurity band. Due to the long-range tail of the Coulomb interaction the Coulomb gap is created at the Fermi energy. For details see [8]. We apply the same numerical procedure to obtain the relaxed pair distribution functions.

First, the positions of $N_d\Omega$ donors and $N_a\Omega$ acceptors are randomly generated in a cubic sample with the volume Ω. The single-particle energy of E_s, which is needed to bring a positive charge from infinity to a donor site z_s without simultaneous rearrangement of charges on other sites, results from the relation

$$E_s\{n_k\} = \varphi_s + \frac{e^2}{4\pi\varepsilon_0\varepsilon_s} \sum_{s';s'\neq s} \frac{n_{s'}e^{-z_{ss'}/d_d}}{z_{ss'}}. \tag{24}$$

$\{n_k\}$ is a set of occupation numbers, $n_s \in \{0, 1\}$, $\sum_s n_s = N_d^+\Omega$. The potential φ_s arises from the fixed charges on the acceptor sites. The Coulomb interaction is screened by the free carriers. We consider our sample as an elementary cell of a periodically repeated lattice and assume that the interaction energy of two sites is determined by the shortest distance between them within this repeated lattice,

$$z_{ss'}^2 = \sum_{\gamma=1}^{3} \left(\min\left\{ \left| z_{\gamma,s} - z_{\gamma,s'} \right|, L - \left| z_{\gamma,s} - z_{\gamma,s'} \right| \right\} \right)^2 \tag{25}$$

where $L^3 = \Omega$. In this way, all sites are equivalent; they seem to be positioned in the middle of the finite sample.

The second step is a relaxation of the positive charge to obtain an equilibrium state at the fixed temperature. In order to speed up the procedure it is useful to relax first to a 'frozen' metastable state [8] which is nearer to the equilibrium than the random distribution. Then thermally activated hops are simulated. One of the charged sites is chosen. The charge can either hop to a neutral site or stay in its position. The probability of the hop from the charged state s into a neutral state s' is given by

$$P_{s \rightarrow s'} = \exp\left(-\beta E_{ss'}\right) \Big/ \left(\sum_{s''} \exp\left(-\beta E_{ss''}\right) + 1\right)^{-1} \tag{26}$$

where $\beta = 1/k_B T$ and the energy

$$E_{ss'} = E_{s'} - E_s - \frac{e^2}{4\pi\varepsilon_0\varepsilon_s} \frac{e^{-z_{ss'}/d_d}}{z_{ss'}}. \tag{27}$$

The third term in (27) comes from the subtraction of the interaction of the charge on site s with itself on site s'. The index s'' runs over neutral states. If the hop is realized, E_s are changed according to actual conditions. The hopping procedure is repeated until the total energy oscillates around some equilibrium position. Then the contribution of the configuration to the pair distribution function average is calculated. The pair distance is given by (25) and the functions are obtained in radial (direction-independent) form. The procedure continues by generation of new impurity positions.

4. Electron mobility

The electron mobility μ is obtained in the relaxation time approximation at the parabolic band in the form

$$\mu = \frac{4e}{3\sqrt{\pi}\,m^*} \int_0^\infty \epsilon^{3/2} \tau(\epsilon) e^{-\epsilon}\, d\epsilon \tag{28}$$

$$\frac{1}{\tau(\epsilon = \hbar^2 k^2/2m^* k_B T)} = \frac{m^* k \Omega}{2\pi\hbar^3} \int_{-1}^{1} (1-x) \left| M\left(k\sqrt{2(1-x)}\right)\right|^2 dx. \tag{29}$$

m^* is the effective mass. The conduction via the impurity band is disregarded. A little rearrangement and substitution of (7) yields

$$\mu = \frac{64\sqrt{2\pi}\,(k_B T)^{3/2}\,(\varepsilon_0\varepsilon_s)^2}{3\sqrt{m^*}e^3} \int_0^\infty \Big\{ \epsilon^3 e^{-\epsilon}\, d\epsilon$$

$$\times \left[\int_0^{2\epsilon} F\left(\frac{2}{\hbar}\sqrt{m^* k_B T x}\right) x\, dx \left(x + \frac{\hbar^2}{4m^* k_B T d_d^2}\right)^{-2} \right]^{-1} \Big\}. \tag{30}$$

5. Results and discussion

If the free carriers play a perceptible role in the screening of the interaction, the mobility is easy to calculate. However, in the case of $n_e \rightarrow 0$ and $d_d \rightarrow \infty$, the singularity in the matrix element must be compensated by a zero limit of $F(k \rightarrow 0) = 0$. This result is difficult to obtain from the MC simulations. The fluctuations in the charge distribution cause oscillations of F in both positive and negative ways.
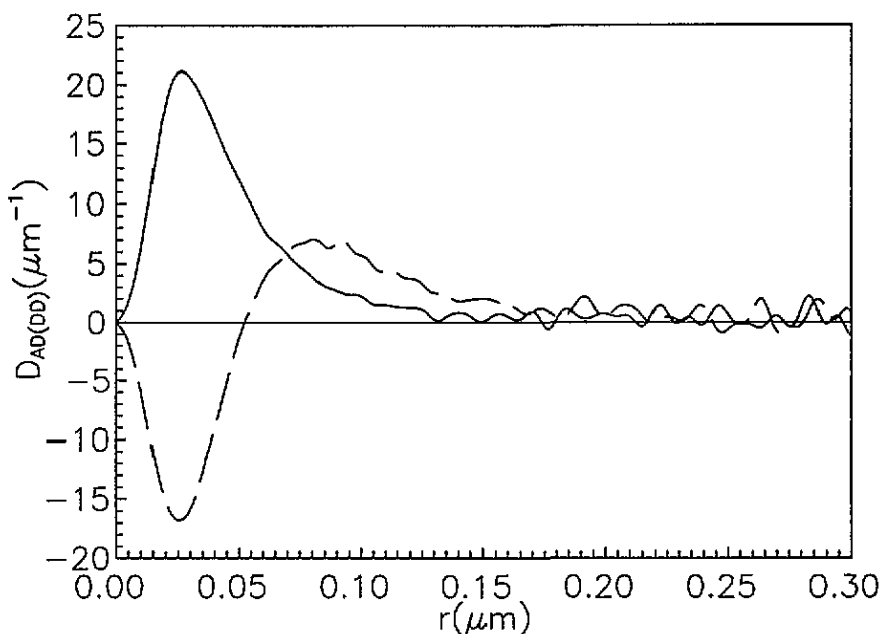
Figure 1. Acceptor–donor (full line) and donor–donor (dashed line) radial distribution functions. $N_a = 5 \times 10^{15}$ cm^{-3}, $N_d = 10^{16}$ cm^{-3}, $n_e = 0$, $T = 1$ K, $N_a\Omega = 5000$, averaged over 310 configurations.

A typical course of the correlation functions can be observed in figure 1. The δ-function peaks resulting from (9) are smoothed by a procedure SMOOFT [9]. In order to make the fluctuations more visible we plot radial distribution functions

$$D_{\text{ad(dd)}}(r) = \frac{4\pi r^2}{\Omega N_d^+} \delta C_{\text{ad(dd)}}(r).$$ (31)

Conforming with (12), D_{dd} does not exhibit a repulsion of a charge to infinity. The rearrangement of the donors creates a Friedel-like oscillation in the charge distribution. A comparison of the total screening functions with (temperature-independent) exponential and dipole correlation can be checked in figure 2.

If the integration in F is performed over the whole volume Ω (see the appendix), the proper zero limit can be obtained. Unfortunately, this procedure does not improve the results. The distribution of the screening charge at a large distance is influenced by an interaction with the charge in the neighbouring cell given by the periodical boundary conditions (25). The screening charge is repulsed from the boundaries to the interior of the volume creating an overscreening of the central charge. Consequently, $F(k)$ is negative at small k.

As we want to check the limit of $F(k \to 0)$, it is useful to plot a function $F(k)/k^2$ to accentuate the small-k behaviour. The plots of this function for the discussed models are collected in figure 3. The influence of charge fluctuations on the MC curves is also demonstrated there. It is evident that none of the analytical models describe the MC simulations properly. Moreover, MC curves indicate a fast decrease at small k.

To check that, we use another possibility to calculate the matrix element. We combine the discrete k as $k = 2\pi n/L$, $n = (n_1, n_2, n_3)$ and use just the form of (4) for the calculation. Then we average over all directions at the same magnitude. The set of the
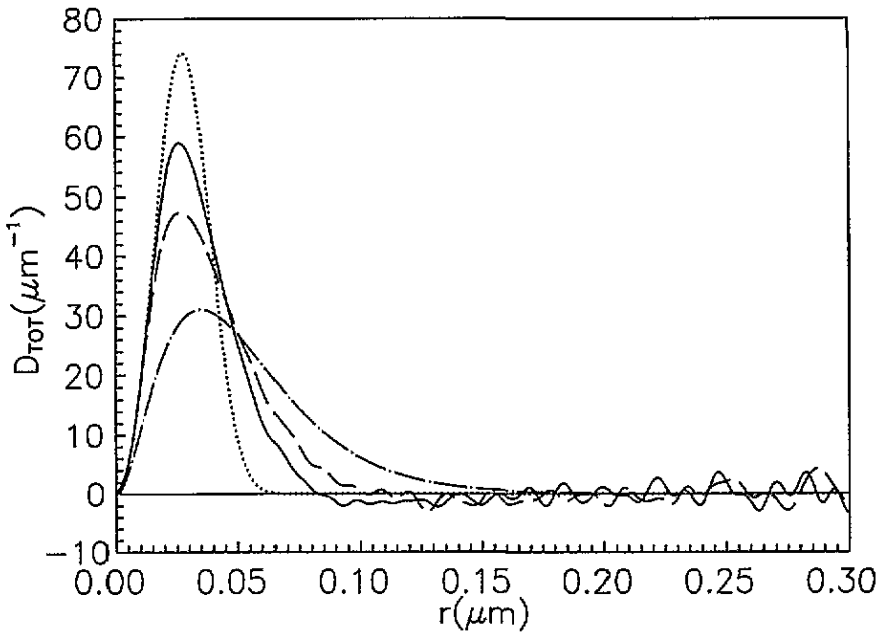
Figure 2. Total radial distribution functions at $T = 1$ K (full) and $T = 10$ K, 260 configurations (dashed) compared with the model of exponential (dash–dotted) and dipole (dotted) correlation. $N_u = 5 \times 10^{15}$ cm^{-3}, $N_d = 10^{16}$ cm^{-3}, $n_e = 0$, $N_a \Omega = 5000$.

Table 1. The set of integer vectors n sorted by the magnitude. The vectors in the boxes correspond to circled points in figure 4.

n	n^2	n	n^2	n	n^2	n	n^2
(1,0,0)	1	(4,2,0)	20	(6,1,0)	37	(5,5,1)	51
(1,1,0)	2	(4,2,1)	21	(6,1,1)	38	(6,4,0)	52
(1,1,1)	3	(3,3,2)	22	(5,3,2)	38	(7,2,0)	53
(2,0,0)	4	(4,2,2)	24	(6,2,0)	40	(6,4,1)	53
(2,1,0)	5	(5,0,0)	25	(5,4,0)	41	(7,2,1)	54
(2,1,1)	6	(4,3,0)	25	(6,2,1)	41	(5,5,2)	54
(2,2,0)	8	(5,1,0)	26	(4,4,3)	41	(6,3,3)	54
(3,0,0)	9	(4,3,1)	26	(5,4,1)	42	(6,4,2)	56
(2,2,1)	9	(5,1,1)	27	(5,3,3)	43	(7,2,2)	57
(3,1,0)	10	(3,3,3)	27	(6,2,2)	44	(5,4,4)	57
(3,1,1)	11	(5,2,0)	29	(6,3,0)	45	(7,3,0)	58
(2,2,2)	12	(4,3,2)	29	(5,4,2)	45	(7,3,1)	59
(3,2,0)	13	(5,2,1)	30	(6,3,1)	46	(5,5,3)	59
(3,2,1)	14	(4,4,0)	32	(4,4,4)	48	(6,5,0)	61
(4,0,0)	16	(4,4,1)	33	(7,0,0)	49	(6,4,3)	61
(4,1,0)	17	(5,2,2)	33	(6,3,2)	49	(6,5,1)	62
(3,2,2)	17	(5,3,0)	34	(7,1,0)	50	(7,3,2)	62
(3,3,0)	18	(5,3,1)	35	(5,5,0)	50	(8,0,0)	64
(4,1,1)	18	(6,0,0)	36	(5,4,3)	50	(8,1,0)	65
(3,3,1)	19	(4,4,2)	36	(7,1,1)	51	(7,4,0)	65

smallest integer vectors n is for demonstration given in table 1. Results for various L

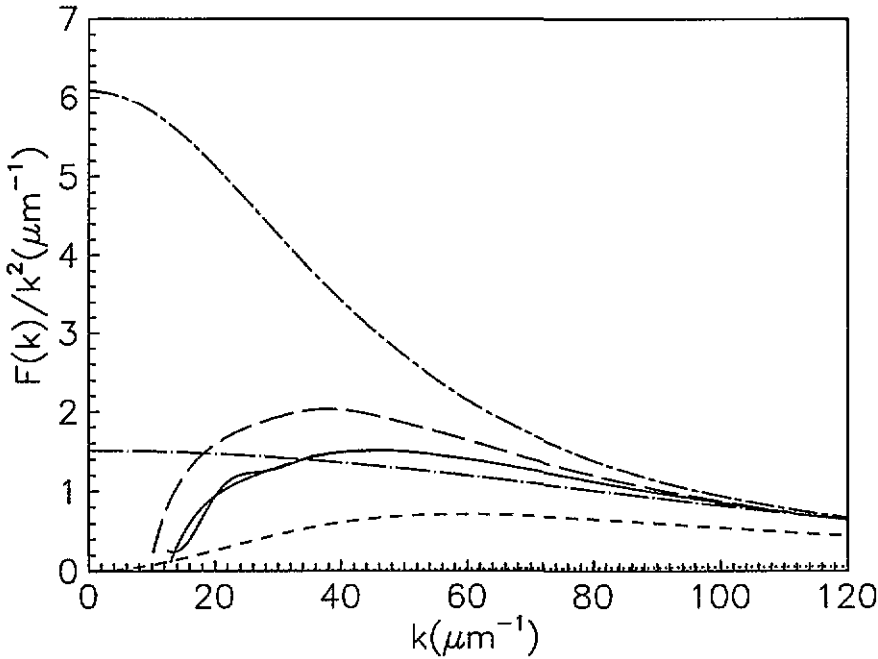**Figure 3.** The function $F(k)/k^2$ for the models mentioned in the text. $N_a = 5 \times 10^{15}$ cm^{-3}, $N_d = 10^{16}$ cm^{-3}, $n_c = 0$. MC simulations 1 K for double averaging (full), 10 K (long dashed), exponential (long–short dashed), dipole (dash–dotted), and for comparison Brooks 1 K (dotted), 10 K (short dashed). The Brooks model curves are given by the form $(N_a + N_d^+)k^2/(k^2 + d_d^{-2})$ which has the same meaning for the electron scattering as $F(k)/k^2$ for the other models.

at $T = 1$ K are shown in figure 4. Other temperatures and compensation rates give similar plots. The circled points correspond to vectors perpendicular to the cube boundaries, $(2, 0, 0)$, $(4, 0, 0)$, $(6, 0, 0)$, $(8, 0, 0)$. They are mostly influenced by the boundary conditions mentioned above and should be abandoned at the mobility calculation. The odd vectors $(3, 0, 0)$, $(5, 0, 0)$, etc., are combined with other general directions which diminish their deviation (see table 1). Also this procedure confirms the zero limit of $F(k)/k^2(k \rightarrow 0)$. Concluding from that we interpolate the interval of small k by a linear dependence $F(k)/k^2(k \rightarrow 0) \propto k$ connected to the MC curve.

This surprising fact entails a significant result for the low-temperature mobility. While all the analytical models discussed above produce either zero or infinity mobility at limit of zero temperature, our numerical calculation gives a constant mobility in this case. The low-temperature proportionalities of the decisive quantities of the discussed models are included in table 2.

A simple criterion for a mobility measurement can be now derived. The decrease of the matrix element is observed for small $k < 2\pi/r_s$, where r_s is an effective screening radius. Applying for simplicity the exponential correlation we obtain $r_s \approx 4/a$. Connecting an effective k_f with temperature we get the criterion which must be fulfilled to measure the effect in the form

$$k_B T \approx \frac{\hbar^2 k_f^2}{2m^*} < \frac{\pi^2 \hbar^2}{2m^*} \left[\frac{\pi \left[2N_a \left(N_d - N_d^+ \right) + \left(N_d^+ \right)^2 \right]}{N_a + N_d^+} \right]^{2/3} . \qquad (32)$$
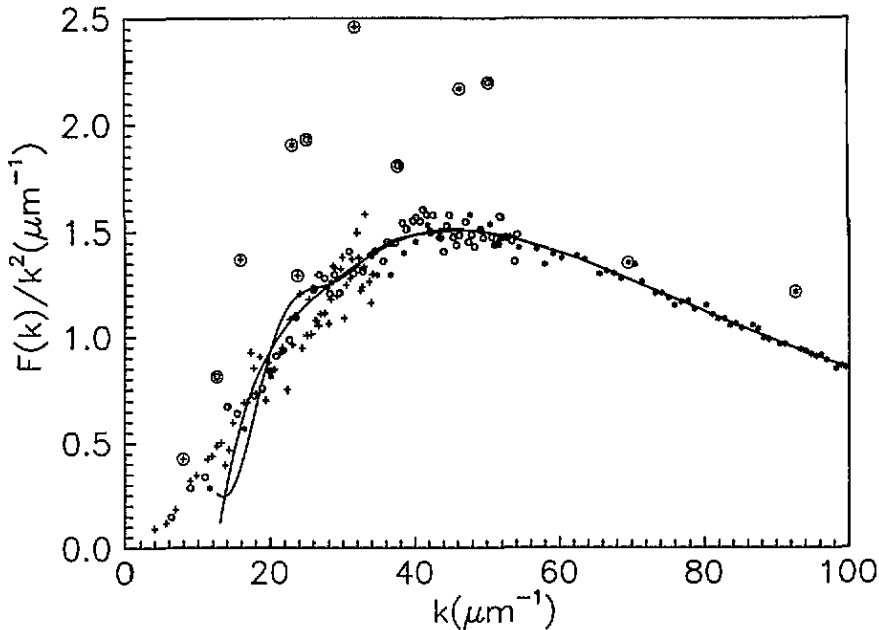
Figure 4. A comparison of $F(k)/k^2$ from MC simulations at $T = 1$ K with discrete k calculation according to (4). (*): $N_a\Omega = 800$, 330 configurations, $L = 0.543$ μm, (o): $N_a\Omega = 5000$, 36 configurations, $L = 1$ μm, (+): $N_a\Omega = 20\,000$, 31 configurations, $L = 1.587$ μm.

Table 2. The proportionality behaviour of $F(k)$, d_d^2 and μ in the limit of low temperature for the models discussed in the text.

Model	$F(k)$	$d_d^2(T)$	$\mu(T)$
Conwell and Weiskopf	constant	constant	$T^{-1/2}$
Brooks and Herring	constant	T	$T^{-5/2}$
Exponential correlation	k^2	∞	$T^{1/2}$
Dipole model	k^2	∞	$T^{1/2}$
Monte Carlo	k^3	∞	constant

Effective-mass dependences of the carrier mobility at two temperatures calculated from (30) are shown in figures 5, 6. Evidently, at $T = 1$ K the dipole model approximates the MC mobility quite well. At $m^* < 0.05m_0$ the error exceeds 50%. Increasing the temperature the MC results deviate in the direction of the exponential correlation.

6. Conclusions

Monte Carlo simulations were used to obtain the pair correlation functions in the system of charged sites in a compensated semiconductor. The donor–donor correlation does not repulse a charge to an infinity. The dipole model is the best to fit the mobility from MC results. Lowering the temperature the selection of screening model influences the electron mobility essentially. The oscillating character of the donor–donor pair correlation function decreases the matrix element for the electron scattering for small k. Consequently constant (non-zero) limit of the electron mobility at zero temperature is obtained. This effect increases the
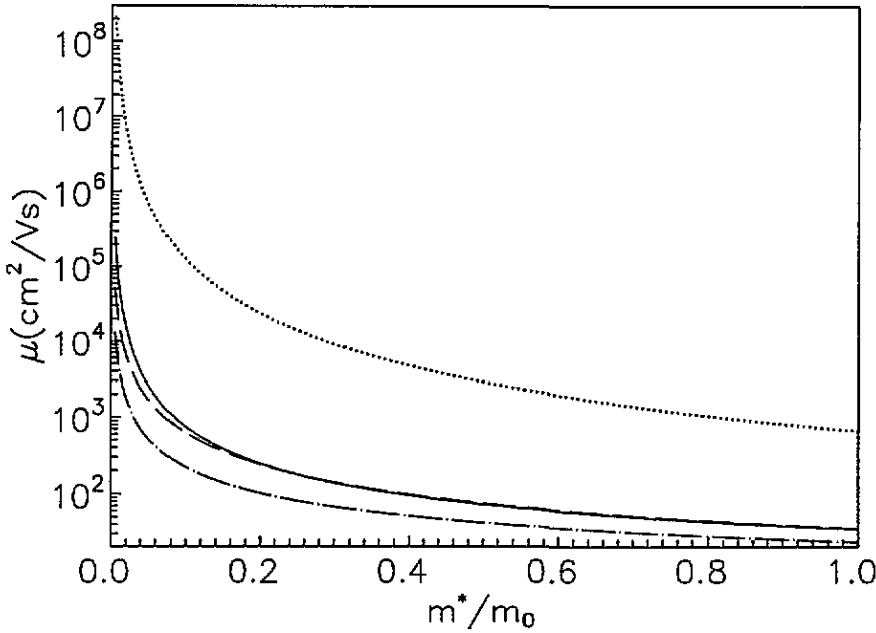
Figure 5. An effective-mass dependence of carrier mobility at $T = 1$ K. MC simulations (full), dipole (dashed), exponential (dash–dotted), Brooks (dotted).
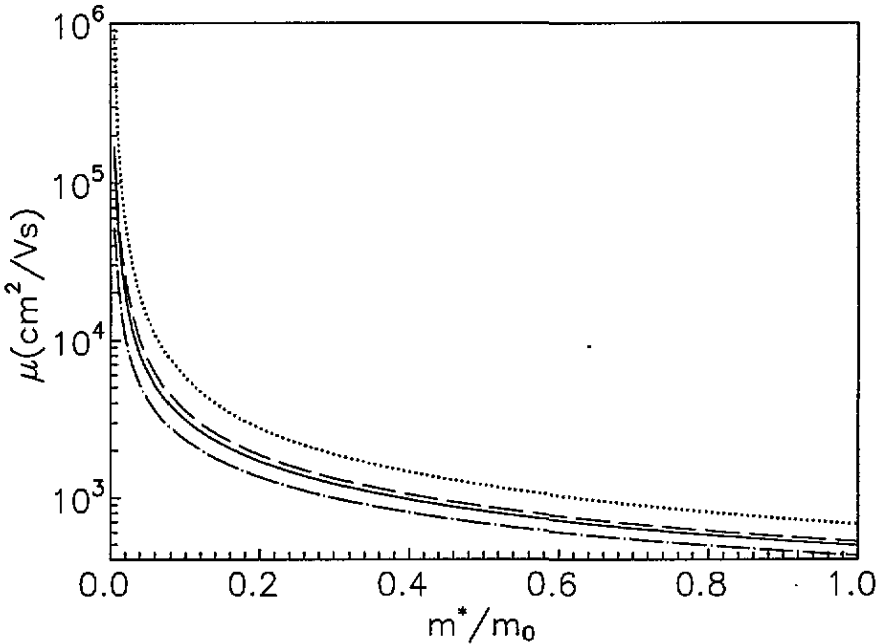

Figure 6. An effective-mass dependence of carrier mobility at $T = 10$ K. MC simulations (full), dipole (dashed), exponential (dash–dotted), Brooks (dotted).

electron mobility at impure semiconductors with a low effective mass at a low temperature as compared to the dipole model. A practical application of the model to bulk semiconductors

is confined by a temperature interval where the free-carrier concentration is large enough to allow the mobility measurement but still sufficiently low to screen the Coulomb interaction.

Acknowledgments

Appendix

The integration in (8) assumes a homogeneous system with spherical symmetry. The MC simulations are performed in a cube. Thus, the precise integration over Ω must be corrected in this respect. This problem is easy to solve using the following transformation

$$\int_\Omega g(r)\,\mathrm{d}^3r = 4\pi \int_0^R r^2 g(r)B(r)\,\mathrm{d}r. \tag{A1}$$

$R = \sqrt{3}L/2$, $g(r)$ is an arbitrary radial function where $r = 0$ in the centre of the cube and B is the correction function expressing a fraction of a spherical surface occurring inside the cube

$$B(r) = \begin{cases} 1 & r \leqslant L/2 \\ (3L - 4r)/2r & L/2 < r \leqslant L/\sqrt{2} \\ f(L/2r) & L/\sqrt{2} < r \leqslant \sqrt{3}L/2 \end{cases} \tag{A2}$$

$$f(y) = \frac{4}{\pi}\left\{3y\left[\tan^{-1}\left(y/\sqrt{1-2y^2}\right) - \pi/4\right] + \pi/2 \right.$$
$$\left. - \tan^{-1}\left(y^2/\sqrt{1-2y^2}\right) - \tan^{-1}\left(1/\sqrt{1-2y^2}\right)\right\}$$

References

[1] Conwell E M and Weisskopf V F 1950 *Phys. Rev.* **77** 388
[2] Brooks H and Herring C 1951 *Phys. Rev.* **83** 879
[3] Falicov L M and Cuevas M 1967 *Phys. Rev.* **164** 1025
[4] Fujita S, Ko C L and Chi J Y 1976 *J. Phys. Chem. Solids* **37** 227
[5] Zubarev D N, Balabanyan G O and Fujita S 1977 *Solid State Commun.* **21** 565
[6] Čápek V 1980 *Czech. J. Phys.* B **30** 684
[7] Shklovskii B I and Efros A L 1984 *Electronic Properties of Doped Semiconductors (Springer Series in Solid-State Sciences 45)* (Berlin: Springer)
[8] Möbius A, Richter M and Drittler B 1992 *Phys. Rev.* B **45** 11 568
[9] Press W H, Flannery B P, Teukolsky S A and Vetterling W T 1986 *Numerical Recipes* (Cambridge: Cambridge University Press)